

## Entanglement entropy, single-particle occupation probabilities, and short-range correlations

Aurel Bulgac *Department of Physics, University of Washington, Seattle, Washington 98195-1560, USA*

(Received 22 March 2022; revised 11 October 2022; accepted 9 June 2023; published 21 June 2023)

For quantum many-body systems with short-range correlations (SRCs), the intimate relationship between their magnitude, the behavior of the single-particle occupation probabilities at momenta larger than the Fermi momentum, and the entanglement entropy is a new qualitative aspect not studied and exploited yet. A large body of recent condensed matter studies indicates that the time evolution of the entanglement entropy describes the nonequilibrium dynamics of isolated and strongly interacting many-body systems, in a manner similar to the Boltzmann entropy, which is strictly defined for dilute and weakly interacting many-body systems. Both theoretical and experimental studies in nuclei and cold atomic gases have shown that the fermion momentum distribution has a generic behavior  $n(k) = C/k^4$  at momenta larger than the Fermi momentum, due to the presence of SRCs, with approximately 20% of the particles having momenta larger than the Fermi momentum. The presence of the long momentum tails in the presence of SRCs changes the textbook relation between the single-particle kinetic energy and occupation probabilities,  $n_{\text{mf}}(k) = 1/\{1 + \exp \beta[\epsilon(k) - \mu]\}$  for momenta very different from the Fermi momentum, particularly for dynamics processes. SRCs induced high-momentum tails of the single-particle occupation probabilities increase the entanglement entropy of fermionic systems, which in its turn affects the dynamics of many nuclear reactions, such as heavy-ion collisions and nuclear fission.

DOI: [10.1103/PhysRevC.107.L061602](https://doi.org/10.1103/PhysRevC.107.L061602)

Short-range correlations (SRCs) are defined as correlations between the constituents of a quantum many-body system at interparticle separations smaller than the average separation between its constituents, which is of order  $1/\sqrt[3]{n(\mathbf{r})}$ , where  $n(\mathbf{r})$  is the number density. Such interparticle separations correspond to particle momenta larger than the local Fermi momentum  $\hbar k_F(\mathbf{r}) = \hbar\sqrt{3\pi^2 n(\mathbf{r})}$ , when the particle motion is essentially unperturbed by the mean field. A great example was discussed by Landau [1], when he discussed the dispersion relation between the (quasi)particle kinetic energy and its momentum  $\epsilon(\mathbf{p})$  in superfluid helium II, where he identified three branches of this spectrum: the phonon branch, the roton branch, and at higher momenta essentially the atom free motion. If the SRCs are strong, their role should appear at relatively small momenta, close to the Fermi momentum  $\hbar k_F$  and the fraction of the quasiparticles with such momenta can be significant. In particular, the single particle occupation probability for Landau quasiparticles is given by the textbook formula [2], apart from the trivial energy shift due the presence of the mean field,

$$n_{\text{mf}}(k) = \frac{1}{1 + \exp \beta[\epsilon(k) - \mu]}, \quad (1)$$

where  $\beta = 1/T$  is the inverse temperature,  $\mu$  is the chemical potential, and  $\epsilon(k) = \hbar^2 k^2/2m$  is the kinetic energy. This formula is valid only in a relatively small energy interval around the Fermi level, strictly speaking only for systems in (quasi)equilibrium and it is in agreement with kinetic theory in the long time limit and quasi-locally for dilute and weakly interacting systems. Its range of validity and accuracy are however not established. Decades long studies of fermion

momentum distribution in nuclei and cold atomic gases, where SRCs are important, require a more sophisticated approach. The relation between the SRCs and the entanglement entropy were discussed recently in Refs. [3–6].

While it appears that only recently it was realized that quantum entanglement and superposition are equivalent concepts [7], with a little bit of effort one can easily convince oneself that the century old two-slit experiment due to Thomas Young, where superposition and coherence (thus entanglement) was crucial, the EPR paradox [8], the entanglement introduced by Schrödinger discussed many times by other authors [9–11], and SRCs in quantum systems where they are present, are intimately related phenomena. Two particles in a many-body system, interacting with forces with a range much shorter than the average particle separation, become naturally entangled as in the situation discussed by Einstein *et al.* [8], when two particles are practically isolated from the rest of the universe and retain the memory of the moment of “creation” of their initial state, a long time after they are fully spatially separated. Many-body systems with SRCs accordingly become entangled at all energies, irrespectively of whether the system is in equilibrium or not, and the measure of entanglement needs to be quantified. The system entanglement entropy directly affects the particle momentum distribution and its nonequilibrium dynamics [3,4]. Isolated quantum systems in a pure state for which either von Neumann or Shannon entropy vanishes, but not necessarily in an equilibrium state, will evolve and its entanglement entropy will naturally in the long run describe their equilibration [12–32], similarly to the Boltzmann entropy for weakly interacting and dilute systems as discussed by Boltzmann [33], Nordheim [34], Uehling and

Uhlenbeck [35]. Entanglement thus becomes a measure of both mean field and short-range correlations as well [4].

The single-particle momentum distribution can be extracted from the one-body density matrix

$$n(\xi|\zeta) = \langle \Phi | \psi^\dagger(\zeta) \psi(\xi) | \Phi \rangle, \quad (2)$$

where  $|\Phi\rangle$  is in general a time-dependent many-body wave function and  $\xi = (\mathbf{r}, \sigma, \tau)$ ,  $\zeta = (\mathbf{r}', \sigma', \tau')$  stand for the spatial, spin, and isospin coordinates. Since the emphasis will be on the spatial properties, the spin and isospin degrees of freedom will be suppressed in ensuing equations. In many-body systems the density matrix typically is characterized by different spatial scales in the coordinates  $\mathbf{R} = (\mathbf{r} + \mathbf{r}')/2$  and  $\mathbf{s} = \mathbf{r} - \mathbf{r}'$ . The momentum distribution, obviously related to the Wigner distribution [36], is defined [37] using Eq. (2) for any many-body wave function

$$n(\mathbf{k}) = \sum_{\sigma, \tau} \int d^3r d^3r' n(\mathbf{r}, \sigma, \tau | \mathbf{r}', \sigma, \tau) e^{-i\mathbf{k} \cdot (\mathbf{r} - \mathbf{r}')}, \quad (3)$$

where  $\int \frac{d^3k}{(2\pi)^3} n(\mathbf{k}) = A$  and  $A = N + Z$  is the atomic number. The properties of the nucleon momentum distribution have been investigated for decades [37–69]. Sartor and Mahaux [40] have shown in 1980 that the momentum distribution of a dilute Fermi system is characterized by the presence of very long momentum tails  $n(k) \propto 1/k^4$  at large momenta. Tan [62–64] later proved that in the momentum interval  $1/|a| \ll k \ll 1/r_0$ , where  $a$  and  $r_0$  are the  $s$ -wave scattering length and effective range respectively, the momentum distribution has the behavior  $n(k) \approx C/k^4$ . Bertsch pointed in 1999 that dilute neutron matter [56,70] is exactly such a system. Subsequent both theoretical and experimental studies for nuclear systems [41,42,46–49,52–55] and for cold fermionic atom systems [56–61,71] confirmed these predictions, even in cases where the interaction has quite a complex character, as in the case of a nuclear tensor interaction. The important conclusion of these studies was that approximately 20% of the spectral strength is found for momenta  $k > k_F$ . As was mentioned by many “A crucial feature of the Tan relations is the fact that they apply to any state of the system, e.g., both to a (normal) Fermi-liquid or to a superfluid state, at zero or at finite temperature and also in a few-body situation.” [56,57,59,62–64]. While nuclear studies were performed for understandable reasons only for the ground states of the systems, the experimental and theoretical results for cold fermionic atoms were obtained both at zero and finite temperatures, confirming Tan’s [62–64] prediction that the  $n(k) = C/k^4$  behavior is in fact generic for strongly interacting many-fermion systems, and thus a feature of such systems in both equilibrium and out of equilibrium. In Refs. [3,4] this aspect is illustrated for the case of highly excited fission fragments, with temperatures well above the critical temperature, where superfluid correlations are absent.

Typically one discusses the angle averaged momentum distribution  $n(k) = \int d\Omega_k n(\mathbf{k})$ , which can be evaluated by constructing the eigenvalues and eigenfunctions

$$\sum_{\zeta} n(\xi|\zeta) \phi_{\alpha}(\zeta) = n_{\alpha} \phi_{\alpha}(\xi), \quad n(\xi|\zeta) = \sum_{\alpha} \phi_{\alpha}(\xi) n_{\alpha} \phi_{\alpha}^*(\zeta) \quad (4)$$

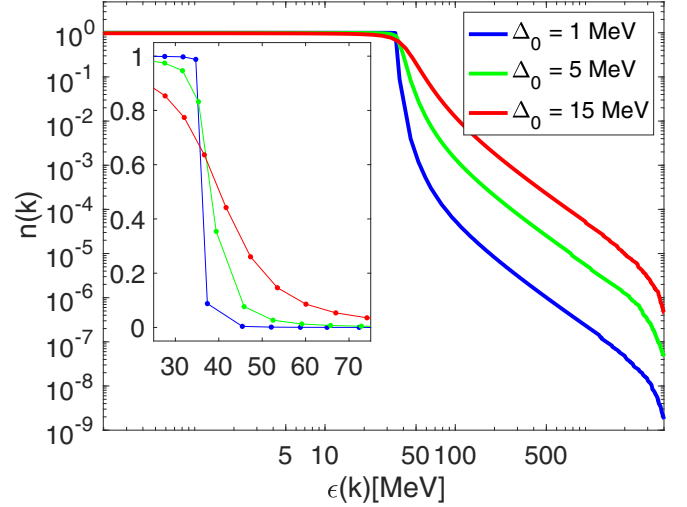


FIG. 1. Typical behavior of the  $s$ -wave canonical occupation probabilities in the case of pairing in a finite nuclear system. Three different amplitudes of the pairing field were considered here  $\Delta_0 = 1, 5, \text{ and } 15 \text{ MeV}$  [4], the last one comparable to the strength of the pairing field in the unitary limit [56]. For  $\epsilon(k) > 75 \text{ MeV}$  the momentum occupation probabilities have the behavior  $n(k) = C/k^4 \propto 1/[\epsilon(k)]^2$ . The UV cutoff is determined by  $\epsilon(k)$  of the highest canonical state with a wave function located inside the system. The states with  $\epsilon(k)$  beyond the UV cutoff are not expected to be physically relevant [4], as their corresponding canonical occupation probabilities vanish in the continuum limit. In the inset, the occupation probabilities  $n(k)$ , shown in a linear scale, have an expected Bardeen-Cooper-Schrieffer [76].

known as the canonical basis in the case of the mean field Hartree-Fock-Bogoliubov approximation [72] or natural orbitals [73,74] in general and evaluating

$$\epsilon(k) = \left\langle \phi_{\alpha} \left| -\frac{\hbar^2 \Delta}{2m} \right| \phi_{\alpha} \right\rangle = \frac{\hbar^2 \mathbf{k}^2}{2m} \quad (5)$$

and thus relating the occupation probability  $n_{\alpha} = n(k) = n(\epsilon(k))$  with  $\epsilon(k)$ . [Note that obviously, the spectrum of Eq. (4) does not depend on the specific representation, either coordinate, momentum, etc.] In saturating systems, such as nuclei, the magnitude of the wave vector  $\mathbf{k}$  is relatively well defined, up to corrections arising from surface effects [75], and the semiclassical quantization approach reproduces with very good accuracy single-particle energies and shell structure, an approximation going back to Bohr’s model of the hydrogen atom. For superfluid systems, if the pairing potential is local, then there is always a range of the wave vectors  $k$  in which  $n(k) = C/k^4$  [4], see Fig. 1. The presence of the high momentum tails  $n(k) = C/k^4$  is clearly incompatible with Eq. (1), which decays exponentially when  $k \rightarrow \infty$ . Note that

$$n(\mathbf{k}) = \sum_{\alpha, \sigma, \tau} n_{\alpha} |\phi_{\alpha}(\mathbf{k}, \sigma, \tau)|^2, \quad (6)$$

$$\phi_{\alpha}(\mathbf{k}, \sigma, \tau) = \int d^3r e^{-i\mathbf{k} \cdot \mathbf{r}} \phi_{\alpha}(\mathbf{r}, \sigma, \tau). \quad (7)$$

The SRCs, which modify in a qualitative manner the behavior of the dependence of the occupation probabilities as a function of their kinetic energy, lead to significant changes of the entropy. This aspect can be appreciated in a much more “down-to-earth” language. In practice, when increasing the spatial resolution, and thus opening new channels and allowing higher momenta to actively participate in the dynamics, the system will always take advantage of new “open roads” and the wave functions will spread naturally over a larger part of the Hilbert space. The entropy is simply a measure of the available and allowed states into which the system can dynamically evolve. As mentioned in introduction, for isolated quantum many-body system the entanglement entropy describes the nonequilibrium dynamics [12–32], similarly to the Boltzmann entropy [33–35]. As recently discussed, the entanglement entropy is also a natural measure of the complexity of the wave function of a quantum many-body system [4]. The complexity of a many-body wave function  $|\Phi\rangle$  [4] can be quantified by evaluating the orbital entanglement or quantum Boltzmann one-body entropy [3,34,35,77–83]

$$S = -g \sum_{\alpha} [n_{\alpha} \ln n_{\alpha} + (1 - n_{\alpha}) \ln(1 - n_{\alpha})], \quad (8)$$

where the Boltzmann constant is  $k_B = 1$  when the temperature is measured in energy units, and  $g$  is spin-isospin degeneracy factor. The set of occupation numbers  $\{n_{\alpha}, 1 - n_{\alpha}\}$  are known as entanglement spectrum and obviously carry more information than the entanglement entropy [20]. A very transparent derivation of the orbital entanglement entropy for fermion systems was given in Ref. [84] using the decomposition, similar to Schmidt decomposition or tensor of the many-body wave function discussed a long time ago by Coleman [85]:

$$|\Phi\rangle = a_{\alpha}^{\dagger} a_{\alpha} |\Phi\rangle + a_{\alpha} a_{\alpha}^{\dagger} |\Phi\rangle = \sqrt{n_{\alpha}} |\Phi_{\alpha}\rangle + \sqrt{1 - n_{\alpha}} |\Phi_{\bar{\alpha}}\rangle, \quad (9)$$

where  $a_{\alpha}^{\dagger}, a_{\alpha}$  are creation and annihilation fermionic operators. This entropy vanishes exactly for an isolated system in a pure Hartree-Fock wave function, thus noninteracting particles, and it is different from zero only in the presence of residual interactions, both for ground and excited states. Cold fermionic gases where the only interaction is a zero-range is perhaps the most simple example of a strongly interacting system where for any scattering length any exact many-body state has SRCs [62–64] and the entanglement entropy  $S$  (8) is nonvanishing for any state, irrespective of whether a pairing condensate is present or not. In the limit of a dilute system with weak particle interactions the entanglement entropy  $S$  is a very good approximation of the thermodynamic entropy in both classical [33] and quantum semiclassical limits [2,34,35]. This entanglement entropy  $S$  is a measure of the amount of the many-body correlations beyond a pure Slater determinant [4], for which  $S \equiv 0$ . The orbital entanglement entropy  $S$  defined in Eq. (8) is related (though it is not identical) to the Shannon entropy [86] familiar in quantum information science, see a discussion in Ref. [4]. The entanglement entropy never vanishes [86,87] for an interacting system in a pure state, and in particular in its ground state. The set of  $-\ln n_k$  is also known as the entanglement spectrum [20].

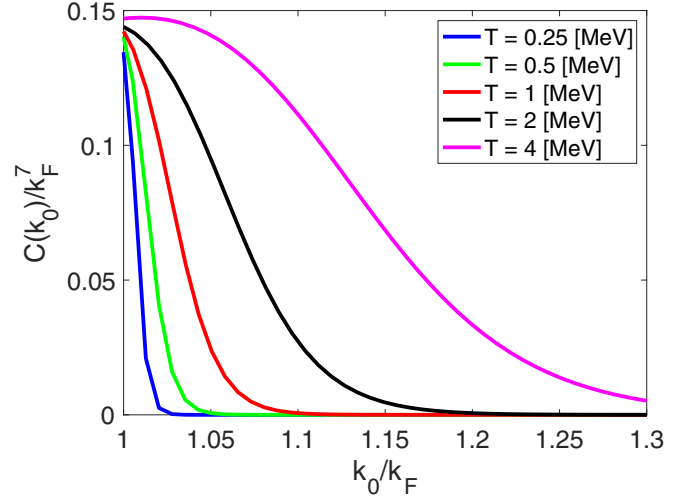


FIG. 2. The dependence of the dimensionless “contact”  $C(k_0)/k_F^7$  on the choice of momentum scale  $k_0$  extracted by imposing the normalization condition Eq. (12) on the occupation probability  $n(k)$ , for a thermal mean field distribution, see Eq. (10) and where the temperature  $\beta = 1/T$ , increases from the lowest to the highest curve.

When accounting for the SRCs the nucleon momentum distribution can be parametrized with a simple model [53]

$$n(k) = \eta(k_0) \begin{cases} n_{\text{mf}}(k), & \text{if } k \leq k_0 \\ n_{\text{mf}}(k_0) k_0^4 / k^4, & \text{if } k_0 < k < \Lambda \end{cases}, \quad (10)$$

$$C(k_0) = \eta(k_0) n_{\text{mf}}(k_0) k_0^4, \quad (11)$$

$$n_0 = g \int_{k < \Lambda} \frac{d^3 k}{(2\pi)^3} n(k) = \frac{g k_F^3}{6\pi^2}, \quad (12)$$

where  $C(k_0)$  the “contact” introduced by Tan [62–64] and  $n_0 \approx 0.16 \text{ fm}^{-3}$  is the saturation density of symmetric nuclear matter. The SRCs part of the momentum distribution  $n(k)$  is clearly a beyond mean field feature in nature. Since so far no argument has been suggested in literature that a discontinuity of  $n(k)$  at  $k_0$  might occur, it is reasonable to assume that  $n(k)$  is continuous and thus there is a simple interpretation of the contact  $C(k_0) = \eta(k_0) n_{\text{mf}}(k_0) k_0^4$  in terms of a single parameter  $k_0$ , see Fig. 2. The presence of a cusp at  $k_0$  in the adopted parametrization of  $n(k)$  introduces only relatively small numerical corrections. The normalization constant  $\eta(k_0)$ , which characterizes the depletion of the Fermi sea due to residual interactions, is obtained from the condition Eq. (12), see Fig. 3,

$$\eta(k_0) = \frac{\int_0^{\Lambda} dk k^2 n_{\text{mf}}(k)}{k_0^3 n_{\text{mf}}(k_0) + \int_0^{k_0} dk k^2 n_{\text{mf}}(k)}. \quad (13)$$

Assuming that  $\Lambda = \infty$  and

$$n_0 = g \int \frac{d^3 k}{(2\pi)^3} n_{\text{mf}}(k), \quad (14)$$

a lower limit for  $\eta(k_0)$  can be obtained in the case of a free Fermi gas at zero temperature by choosing  $k_0 = k_F$ . One can now evaluate the fraction of the particles with momenta

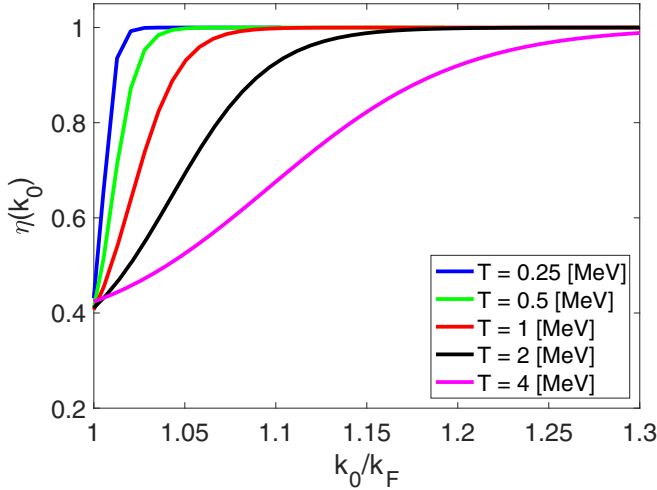


FIG. 3. The dependence of  $\eta(k_0)$  on the choice of momentum scale  $k_0$  extracted from Eq. (13), for different temperatures when  $n_{\text{mf}}(k)$  is a thermal distribution for free fermion gas. For  $k_0 > 1.05k_f$  the temperature decreases from the lowest to the highest curve.

greater than  $k_0$ , see Fig. 4,

$$\frac{n(k > k_0)}{n_0} = \frac{3\eta n_{\text{mf}}(k_0)k_0^3}{k_F^3} = \frac{3C(k_0)}{k_0 k_F^3}, \quad (15)$$

which can reach quite large values. It is not my goal here to select the best choice for the mean field momentum probability distribution, as that should be decided in accurate microscopic calculation, specific for various systems [47–49,51,52,55–57,59–61,88,89].

The UV-momentum cutoff  $\Lambda$  of the momentum distribution  $n(k)$  is effective field theory in nature and is determined by the internal structure of the nucleons. In the limit  $k_0 \rightarrow \infty$  the “contact”  $C$  naturally vanishes. The specific value of the “contact”  $C$  is defined by the temperature  $T$ , the specific system under consideration, and the system specific momentum scale  $k_0$  [40–42,46–49,51–53,55,58,60–64,88–92].

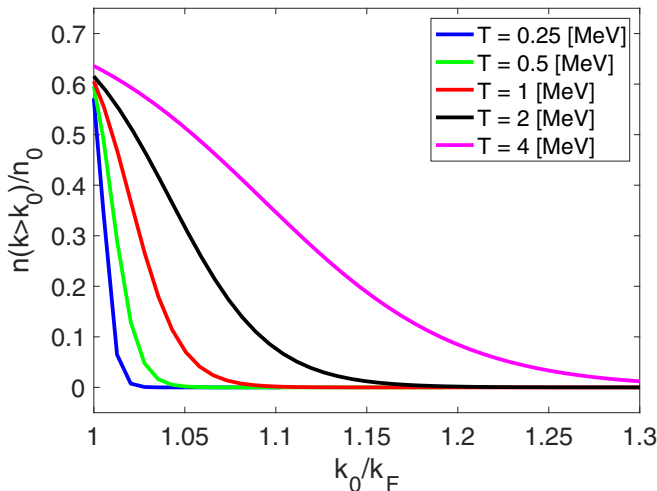


FIG. 4. The fraction of the particles  $n(k > k_0)/n_0$  with momenta  $k \geq k_0$ , where  $n(k) \propto 1/k^4$ . The curves rank by temperature.

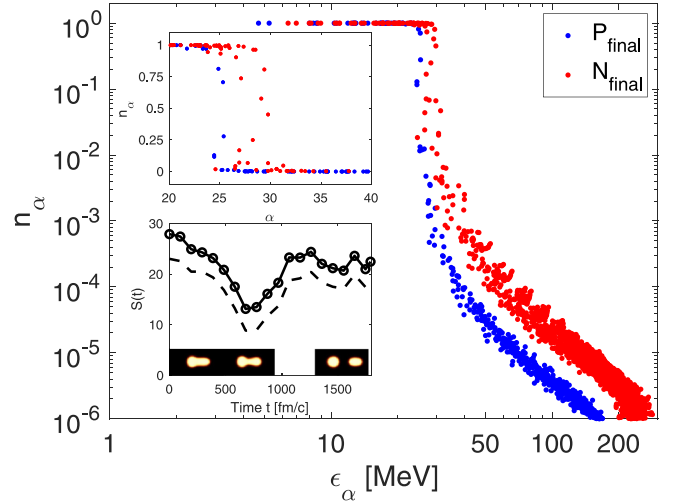


FIG. 5. The final proton and neutron canonical occupation probabilities  $n_\alpha = n(k)$  extracted from the TDDFT extended to superfluid systems treatment of induced fission reaction  $^{235}\text{U}(n, f)$  as a function of  $\epsilon_\alpha = \epsilon(k)$ . The upper inset shows a small energy interval near the Fermi level. Above  $\epsilon_\alpha \approx 50$  MeV one can see a clear power law behavior compatible with theory prediction  $n(k) \propto 1/[\epsilon(k)]^2$ . The initial state was the compound nucleus close to the top of the outer fission barrier at  $t = 0$  fm/c and in the final state the fission fragments are spatially separated by  $\approx 30$  fm at  $t = 1700$  fm/c [4]. The nonequilibrium time-evolution of the orbital entanglement entropy  $S(t)$  is shown in the lower inset, with solid and dashed lines corresponding to no nucleon number projections and with nucleon number projections, respectively [4].

The momentum distribution  $n(k)$  has thus two components, the mean field and the SRCs components, which can be clearly identified experimentally [53,55,58] by identifying the regime  $k_0 < k < \Lambda$ , where  $n(k) \approx C(k_0)/k^4$  is valid. Below  $k < k_0$  the  $n(k)$  can be then identified with a mean field contribution, up to the overall renormalization constant  $\eta(k_0) \leq 1$ . The constant  $\eta(k_0)$  is uniquely determined by the normalization condition Eq. (12) and the mean field component  $n_{\text{mf}}(k)$ , which is determined in a typical mean field or density functional theory (DFT) [93,94]. The momentum distribution  $n(k)$  depends on a single parameter  $k_0 > k_f$ , that can be determined either experimentally or from DFT with a sufficiently large UV-momentum cutoff or from another accurate many-body calculation, when pairing correlations are also taken into account [3,95].

In the classic monograph [2] there is a somewhat hard to interpret sentence, stating that the dependence of the occupation probabilities on the quasiparticle energies  $\epsilon$  is a *very complicated implicit definition of  $n(\epsilon)$*  (see Eq. (2.6) in Ref. [2] and the corresponding explanations), whereas  $n(\epsilon)$  is clearly a well-defined function of  $\epsilon$ , see Eq. (1). In Fig. 5 I show the dependence of the canonical occupation probabilities  $n_\alpha = n(\epsilon(k))$  in case of induced fission  $^{235}\text{U}(n, f)$ , extracted from the time-dependent DFT (TDDFT) approach extended to superfluid systems and applied to this nonequilibrium process [96–100]. These results show the momentum distribution of two hot emerging fission fragments, with a separation in space  $\approx 30$  fm, and at temperatures larger than the critical

TABLE I. The values of the ratio of the entropy of the system, in the presence of SRCs, evaluated with Eq. (10), over the entropy evaluated in pure mean field approximation evaluated with Eq. (1), for different values of the momentum scale  $k_0$ , is shown in columns 2–6.

	$\frac{k_0}{k_F} = 1.3$	$\frac{k_0}{k_F} = 1.2$	$\frac{k_0}{k_F} = 1.1$	$\frac{k_0}{k_F} = 1.05$	$\frac{k_0}{k_F} = 1$
$T = 0.25$ MeV	1	1	1	1	124.6
$T = 0.5$ MeV	1	1	1	2.18	60
$T = 1$ MeV	1	1	1.28	8.92	29.8
$T = 2$ MeV	1	1.11	4.01	10.48	14.9
$T = 4$ MeV	1.27	2.41	5.57	6.81	7.60

temperature  $T_c \approx 0.5$  MeV for which the pairing gaps vanish, and which demonstrate the clear presence of proton-proton and neutron-neutron SRCs [3]. In the dynamics of isolated systems the time evolution of the entanglement entropy plays the role of thermodynamic entropy for local observables [12–14], is shown in the lower inset of Fig. 5. Note that at the initial time the nucleus is at zero temperature, but the entanglement entropy does not vanish. For more details see Ref. [4]. In these calculations nucleon momenta up to  $p_{\text{cut}} = \hbar\pi/dx \approx 600$  MeV/c (where the spatial resolution is  $dx = 1$  fm) are present. According to the prevalent interpretation of time-dependent mean field treatment of many fermion systems, only long-range correlations should be present, which obviously is not the case in TDDFT extended to superfluid systems [3,4,96,97]. This dependence of  $n(k)$  on  $\epsilon(k)$ , where the long-momentum tails are present, is indeed a complicated implicit definition of the canonical occupation probabilities. The canonical basis set is the unique (gauge invariant) and at the same the minimal set of single-particle states to represent a many-body wave function [4,73,74,85,101]. This clarifies perhaps for the first time the meaning of the sentence quoted above and an equivalent of which I could not find in literature. The presence of the infrared knee at  $\epsilon_\alpha \approx 40$  MeV is unequivocally a qualitative new feature, absent from the textbook definition [2] of a quasiequilibrium distribution  $n(\epsilon)$ .

After a cursory analysis of Eq. (8), one is lead to the conclusion that due to the presence of the SRCs contribution this entanglement entropy likely exceeds in value the corresponding entanglement mean field entropy, see Table I. The SRCs contribution to  $n(k)$  has a very long power law tail, which would lead to  $\eta(k_0) < 1$ , see Fig. 3, and thus to an expected depletion of the occupation probabilities of the low-momentum states  $k < k_0$ , even at very low temperatures. This occupation probability depletion of the states with  $k < k_0$  alone would lead to an increase of the corresponding contribution of these states to the entropy density of the system. At the same time, the long tails of the momentum distribution for  $k > k_0$  would lead to a further increase of the entropy density, when compared to the mean field value. Since  $\Lambda \gg k_0$ , the effect of considering the internal nucleon structure have likely a relatively small effect on the entropy, which is well converged when  $n(\Lambda) \approx 10^{-7}$ . Upon performing a projection on exact proton and neutron numbers the many-body wave function is an exponentially large sum of Slater determinants (a typical shell-model or configuration interaction many-body wave function), the canonical/natural orbital occupation probabilities remain largely unchanged [4,5] and thus the particle

projected many-body wave function retains a very high degree of entanglement. This many-body wave function is solution of the quantum equivalent of the semiclassical Boltzmann equation [4].

Pairing correlations alone lead to  $1/k^4$  tails in the momentum distribution at all temperatures [3,95]. Moreover, the dynamical pairing effects, namely the presence of a pairing field, but the absence of a true pairing condensate at temperatures higher than the critical temperature, lead to the occupation of high-momentum states with  $k > k_0$  [3,99,100], even in time-dependent processes and for intrinsic excitation energies of nuclei corresponding to temperatures above the critical temperature. Since these pairing correlations in current nuclear simulations take into account only the  $nn$  and  $pp$  correlations [3], the effects of  $np$  SRCs can be included in dynamical calculations by an extension of time-dependent DFT described in Ref. [3], are expected to be significantly larger. Since entanglement entropy and many-body level density control the dynamics of an isolated quantum system [12–14], the level density in the presence of SRCs exceeds the level density of the system in a simpler mean field approximation. The possibility that the momentum distribution may be time-dependent as well was not explicitly discussed here, only indirectly illustrated in the lower inset in Fig. 5, it was definitely observed in time-dependent microscopic quantum studies [3–5]. The highly nonequilibrium nuclear fission  $^{235}\text{U}(n, f)$  illustrated here and in Refs. [4,5] in arguably the largest many-body system studied so far [15–32], with aspects related to the widely studied topics of Hilbert space and many-body localization. The presence of SRCs lead to qualitative changes of the entanglement properties, the complexity of the many-body wave functions, the single-particle occupation probabilities, and the dynamics of many-body systems [3–5,99,100,102–106]. Nuclear and cold atom systems present a unique opportunity to study time-dependent nonequilibrium and entanglement properties of strongly interacting fermions.

The funding from the US DOE, Office of Science, Grant No. DE-FG02-97ER41014 and also the support provided in part by NNSA cooperative Agreement No. DE-NA0003841 is greatly appreciated. This research used resources of the Oak Ridge Leadership Computing Facility, which is a U.S. DOE Office of Science User Facility supported under Contract No. DE-AC05-00OR22725. I thank M. Kafker and I. Abdurrahman for the help in computing the results presented in Figs. 1 and 5.

- [1] L. D. Landau, On the theory of superfluidity of helium II, *J. Phys. USSR* **11**, 91 (1947).
- [2] A. A. Abrikosov, L. P. Gorkov, and I. E. Dzyaloshinski, *Methods of Quantum Field Theory in Statistical Physics* (Prentice Hall, Englewood Cliffs, NJ, USA, 1963).
- [3] A. Bulgac, Pure quantum extension of the semiclassical Boltzmann-Uehling-Uhlenbeck equation, *Phys. Rev. C* **105**, L021601 (2022).
- [4] A. Bulgac, M. Kafker, and I. Abdurrahman, Measures of complexity and entanglement in many-fermion systems, *Phys. Rev. C* **107**, 044318 (2023).
- [5] A. Bulgac, New developments in fission studies within the time-dependent density functional theory framework, *EPJ Web of Conferences*, **284**, 04001 (2023).
- [6] Ehoud Pazy, Entanglement entropy between short range correlations and the Fermi sea in nuclear structure, *Phys. Rev. C* **107**, 054308 (2023).
- [7] G. Aubrun, L. Lami, C. Palazuelos, and M. Plávala, Entanglement and Superposition Are Equivalent Concepts in Any Physical Theory, *Phys. Rev. Lett.* **128**, 160402 (2022).
- [8] A. Einstein, B. Podolsky, and N. Rosen, Can quantum-mechanical description of physical reality be considered complete? *Phys. Rev.* **47**, 777 (1935).
- [9] E. Schrödinger, Die gegenwärtige situation in der quantenmechanik, *Naturwissenschaften* **23**, 807 (1935).
- [10] J. S. Bell, On the Eistein Podolsky Rosen paradox, *Phys. Phys. Fiz.* **1**, 195 (1964).
- [11] D. J. Wineland, Nobel lecture: Superposition, entanglement, and raising Schrödinger's cat, *Rev. Mod. Phys.* **85**, 1103 (2013).
- [12] P. Calabrese and J. Cardy, Evolution of entanglement entropy in one-dimensional systems, *J. Stat. Mech.* (2005) P04010.
- [13] P. Calabrese and J. Cardy, Time Dependence of Correlation Functions Following a Quantum Quench, *Phys. Rev. Lett.* **96**, 136801 (2006).
- [14] V. Alba and P. Calabrese, Entanglement and thermodynamics after a quantum quench in integrable systems, *Proc. Natl. Acad. Sci. USA* **114**, 7947 (2017).
- [15] G. J. Milburn, J. Corney, E. M. Wright, and D. F. Walls, Quantum dynamics of an atomic Bose-Einstein condensate in a double-well potential, *Phys. Rev. A* **55**, 4318 (1997).
- [16] G. Vidal, J. I. Latorre, E. Rico, and A. Kitaev, Entanglement in Quantum Critical Phenomena, *Phys. Rev. Lett.* **90**, 227902 (2003).
- [17] V. E. Korepin, Universality of Entropy Scaling in One Dimensional Gapless Models, *Phys. Rev. Lett.* **92**, 096402 (2004).
- [18] A. Kitaev and J. Preskill, Topological Entanglement Entropy, *Phys. Rev. Lett.* **96**, 110404 (2006).
- [19] M. Levin and X.-G. Wen, Detecting Topological Order in a Ground State Wave Function, *Phys. Rev. Lett.* **96**, 110405 (2006).
- [20] H. Li and F. D. M. Haldane, Entanglement Spectrum as a Generalization of Entanglement Entropy: Identification of Topological Order in Non-Abelian Fractional Quantum Hall Effect States, *Phys. Rev. Lett.* **101**, 010504 (2008).
- [21] M. Chuchem, K. Smith-Mannschott, M. Hiller, T. Kottos, A. Vardi, and D. Cohen, Quantum dynamics in the bosonic Josephson junction, *Phys. Rev. A* **82**, 053617 (2010).
- [22] A. Pal and D. A. Huse, Many-body localization phase transition, *Phys. Rev. B* **82**, 174411 (2010).
- [23] J. H. Bardarson, F. Pollmann, and J. E. Moore, Unbounded Growth of Entanglement in Models of Many-Body Localization, *Phys. Rev. Lett.* **109**, 017202 (2012).
- [24] D. Cohen, V. I. Yukalov, and K. Ziegler, Hilbert-space localization in closed quantum systems, *Phys. Rev. A* **93**, 042101 (2016).
- [25] D. A. Abanin, E. Altman, I. Bloch, and M. Serbyn, Colloquium: Many-body localization, thermalization, and entanglement, *Rev. Mod. Phys.* **91**, 021001 (2019).
- [26] S. Sinha and S. Sinha, Chaos and Quantum Scars in Bose-Josephson Junction Coupled to a Bosonic Mode, *Phys. Rev. Lett.* **125**, 134101 (2020).
- [27] S. Wimberger, G. Manganelli, A. Brollo, and L. Salasnich, Finite-size effects in a bosonic Josephson junction, *Phys. Rev. A* **103**, 023326 (2021).
- [28] A. Del Maestro, H. Barghathi, and B. Rosenow, Equivalence of spatial and particle entanglement growth after a quantum quench, *Phys. Rev. B* **104**, 195101 (2021).
- [29] A. Del Maestro, H. Barghathi, and B. Rosenow, Measuring postquench entanglement entropy through density correlations, *Phys. Rev. Res.* **4**, L022023 (2022).
- [30] Q. Liu and K. Ziegler, Entanglement transition through Hilbert-space localization, *Phys. Rev. A* **107**, 012413 (2023).
- [31] N. Mueller, T. V. Zache, and R. Ott, Thermalization of Gauge Theories from their Entanglement Spectrum, *Phys. Rev. Lett.* **129**, 011601 (2022).
- [32] J. T. Schneider, S. J. Thomson, and L. Sanchez-Palencia, Entanglement spectrum and quantum phase diagram of the long-range XXZ chain, *Phys. Rev. B* **106**, 014306 (2022).
- [33] L. Boltzmann, Weitere studien über das wärmegleichgewicht unter gasmolekülen, *Sitzungsberichte Akad. Wiss.* **66**, 275 (1872).
- [34] L. W. Nordheim, On the kinetic method in the new statistics and its application in the electron theory of conductivity, *Proc. R. Soc. London A* **A119**, 689 (1928).
- [35] E. A. Uehling and G. E. Uhlenbeck, Transport phenomena in Einstein-Bose and Fermi-Dirac gases. I, *Phys. Rev.* **43**, 552 (1933).
- [36] E. Wigner, On the quantum correction for thermodynamic equilibrium, *Phys. Rev.* **40**, 749 (1932).
- [37] O. Benhar, V. R. Pandharipande, and S. C. Pieper, Electron-scattering studies of correlations in nuclei, *Rev. Mod. Phys.* **65**, 817 (1993).
- [38] J. S. Levinger, The high energy nuclear photoeffect, *Phys. Rev.* **84**, 43 (1951).
- [39] J. M. Cavedon, B. Frois, D. Goutte, M. Huet, Ph. Leconte, C. N. Papanicolas, X. H. Phan, S. K. Platchkov, S. Williamson, W. Boeglin, and I. Sick, Is the Shell-Model Concept Relevant for the Nuclear Interior? *Phys. Rev. Lett.* **49**, 978 (1982).
- [40] R. Sartor and C. Mahaux, Self-energy, momentum distribution, and effective masses of a dilute Fermi gas, *Phys. Rev. C* **21**, 1546 (1980).
- [41] L.L. Frankfurt and M.I. Strikman, High-energy phenomena, short-range nuclear structure and QCD, *Phys. Rep.* **76**, 215 (1981).
- [42] L. Frankfurt and M. Strikman, Hard nuclear processes and microscopic nuclear structure, *Phys. Rep.* **160**, 235 (1988).
- [43] V. R. Pandharipande, I. Sick, and P. K. A. deWitt Huberts, Independent particle motion and correlations in fermion systems, *Rev. Mod. Phys.* **69**, 981 (1997).

- [44] E. N. M. Quint, J. F. J. van den Brand, J. W. A. den Herder, E. Jans, P. H. M. Keizer, L. Lapikás, G. van der Steenhoven, P. K. A. de Witt Huberts, S. Klein, P. Grabmayr, G. J. Wagner, H. Nann, B. Frois, and D. Goutte, Relative  $3s$  Spectroscopic Strength in  $^{206}\text{Pb}$  and  $^{208}\text{Pb}$  Studied with the  $(e, e'p)$  Knockout Reaction, *Phys. Rev. Lett.* **57**, 186 (1986).
- [45] E. N. M. Quint, B. M. Barnett, A. M. van den Berg, J. F. J. van den Brand, H. Clement, R. Ent, B. Frois, D. Goutte, P. Grabmayr, J. W. A. den Herder, E. Jans, G. J. Kramer, J. B. J. M. Lanen, L. Lapikás, H. Nann, G. van der Steenhoven, G. J. Wagner, and P. K. A. de Witt Huberts, Evidence for Partial Occupancy of the  $3s_{1/2}$  Proton Orbit in  $^{208}\text{Pb}$ , *Phys. Rev. Lett.* **58**, 1088 (1987).
- [46] C. Ciofi degli Atti and S. Simula, Realistic model of the nucleon spectral function in few- and many-nucleon systems, *Phys. Rev. C* **53**, 1689 (1996).
- [47] E. Piassetzky, M. Sargsian, L. Frankfurt, M. Strikman, and J. W. Watson, Evidence for Strong Dominance of Proton-Neutron Correlations in Nuclei, *Phys. Rev. Lett.* **97**, 162504 (2006).
- [48] M. M. Sargsian, T. V. Abrahamyan, M. I. Strikman, and L. L. Frankfurt, Exclusive electrodisintegration of  $^3\text{He}$  at high  $Q^2$ . II. Decay function formalism, *Phys. Rev. C* **71**, 044615 (2005).
- [49] R. Schiavilla, R. B. Wiringa, S. C. Pieper, and J. Carlson, Tensor Forces and the Ground-State Structure of Nuclei, *Phys. Rev. Lett.* **98**, 132501 (2007).
- [50] C. Biscontí, F. Arias de Saavedra, and G. Co', Momentum distributions and spectroscopic factors of doubly closed shell nuclei in correlated basis function theory, *Phys. Rev. C* **75**, 054302 (2007).
- [51] J. Arrington, D.W. Higinbotham, G. Rosner, and M. Sargsian, Hard probes of short-range nucleon–nucleon correlations, *Prog. Part. Nucl. Phys.* **67**, 898 (2012).
- [52] M. M. Sargsian, New properties of the high-momentum distribution of nucleons in asymmetric nuclei, *Phys. Rev. C* **89**, 034305 (2014).
- [53] O. Hen *et al.*, Momentum sharing in imbalanced Fermi systems, *Science* **346**, 614 (2014).
- [54] A. Rios, A. Polls, and W. H. Dickhoff, Density and isospin-asymmetry dependence of high-momentum components, *Phys. Rev. C* **89**, 044303 (2014).
- [55] O. Hen, G. A. Miller, E. Piassetzky, and L. B. Weinstein, Nucleon-nucleon correlations, short-lived excitations, and the quarks within, *Rev. Mod. Phys.* **89**, 045002 (2017).
- [56] *The BCS–BEC Crossover and the Unitary Fermi Gas*, Lecture Notes in Physics, Vol. 836, edited by W. Zwerger (Springer-Verlag, Berlin/Heidelberg, 2012).
- [57] E. Braaten, *Universal Relations for Fermions with Large Scattering Length* (Springer, Berlin/Heidelberg, 2012), Chap. 6, pp. 193–231.
- [58] J. T. Stewart, J. P. Gaebler, T. E. Drake, and D. S. Jin, Verification of Universal Relations in a Strongly Interacting Fermi Gas, *Phys. Rev. Lett.* **104**, 235301 (2010).
- [59] Y. Castin and F. Werner, *The Unitary Gas and its Symmetry Properties* (Springer, Berlin/Heidelberg, 2012), Chap. 5.
- [60] E. R. Anderson and J. E. Drut, Pressure, Compressibility, and Contact of the Two-Dimensional Attractive Fermi Gas, *Phys. Rev. Lett.* **115**, 115301 (2015).
- [61] W. J. Porter and J. E. Drut, Tan's contact and the phase distribution of repulsive Fermi gases: Insights from quantum chromodynamics noise analyses, *Phys. Rev. A* **95**, 053619 (2017).
- [62] S. Tan, Energetics of a strongly correlated Fermi gas, *Ann. Phys.* **323**, 2952 (2008).
- [63] S. Tan, Large momentum part of a strongly correlated Fermi gas, *Ann. Phys.* **323**, 2971 (2008).
- [64] S. Tan, Generalized virial theorem and pressure relation for a strongly correlated Fermi gas, *Ann. Phys.* **323**, 2987 (2008).
- [65] Z. X. Yang, X. L. Shang, G. C. Yong, W. Zuo, and Y. Gao, Nucleon momentum distributions in asymmetric nuclear matter, *Phys. Rev. C* **100**, 054325 (2019).
- [66] T. Aumann, C. Barbieri, D. Bazin, C. A. Bertulani, A. Bonaccorso, W. H. Dickhoff, A. Gade, M. Gómez-Ramos, B. P. Kay, A. M. Moro, T. Nakamura, A. Obertelli, K. Ogata, S. Paschalis, and T. Uesaka, Quenching of single-particle strength from direct reactions with stable and rare-isotope beams, *Prog. Part. Nucl. Phys.* **118**, 103847 (2021).
- [67] A. J. Tropiano, S. K. Bogner, and R. J. Furnstahl, Short-range correlation physics at low renormalization group resolution, *Phys. Rev. C* **104**, 034311 (2021).
- [68] A. J. Tropiano, S. K. Bogner, R. J. Furnstahl, and M. A. Hisham, Quasi-deuteron model at low renormalization group resolution, *Phys. Rev. C* **106**, 024324 (2022).
- [69] J. Arrington, N. Fomin, and A. Schmidt, Progress in understanding short-range structure in nuclei: An experimental perspective, *Annu. Rev. Nucl. Part. Sci.* **72**, 307 (2022).
- [70] G. A. Baker, Neutron matter model, *Phys. Rev. C* **60**, 054311 (1999).
- [71] El. V. H. Doggen and J. J. Kinnunen, Momentum-resolved spectroscopy of a Fermi liquid, *Sci. Rep.* **5**, 9539 (2015).
- [72] P. Ring and P. Schuck, *The Nuclear Many-Body Problem*, 1st ed. (Springer-Verlag, Berlin/Heidelberg/New York, 2004).
- [73] P.-O. Löwdin and H. Shull, Natural orbitals in the quantum theory of two-electron systems, *Phys. Rev.* **101**, 1730 (1956).
- [74] P.-O. Löwdin, Quantum theory of cohesive properties of solids, *Adv. Phys.* **5**, 1 (1956).
- [75] M. Brack and R. K. Bhaduri, *Semiclassical Physics* (Addison-Wesley, Reading, MA, 1997).
- [76] J. Bardeen, L. N. Cooper, and J. R. Schrieffer, Theory of superconductivity, *Phys. Rev.* **108**, 1175 (1957).
- [77] I. Klich, Lower entropy bounds and particle number fluctuations in a Fermi sea, *J. Phys. A: Math. Gen.* **39**, L85 (2006).
- [78] L. Amico, R. Fazio, A. Osterloh, and V. Vedral, Entanglement in many-body systems, *Rev. Mod. Phys.* **80**, 517 (2008).
- [79] R. Horodecki, P. Horodecki, M. Horodecki, and K. Horodecki, Quantum entanglement, *Rev. Mod. Phys.* **81**, 865 (2009).
- [80] M. Haque, O. S. Zozulya, and K. Schouten, Entanglement between particle partitions in itinerant many-particle states, *J. Phys. A: Math. Theor.* **42**, 504012 (2009).
- [81] J. Eisert, M. Cramer, and M. B. Plenio, Colloquium: Area laws for the entanglement entropy, *Rev. Mod. Phys.* **82**, 277 (2010).
- [82] K. Boguslawski and P. Tecmer, Orbital entanglement in quantum chemistry, *Int. J. Quantum Chem.* **115**, 1289 (2015).
- [83] C. Robin, M. J. Savage, and N. Pillet, Entanglement rearrangement in self-consistent nuclear structure calculations, *Phys. Rev. C* **103**, 034325 (2021).
- [84] N. Gigena and R. Rossignoli, Entanglement in fermion systems, *Phys. Rev. A* **92**, 042326 (2015).
- [85] A. J. Coleman, Structure of fermion density matrices, *Rev. Mod. Phys.* **35**, 668 (1963).
- [86] I. Bengtsson and K. Życzkowski, *Geometry of Quantum States (An Introduction to Quantum Entanglement)*, 2nd ed. (Cambridge University Press, Cambridge, 2017).

- [87] M. Srednicki, Entropy and Area, *Phys. Rev. Lett.* **71**, 666 (1993).
- [88] J. E. Drut, T. A. Lähde, and T. Ten, Momentum Distribution and Contact of the Unitary Fermi Gas, *Phys. Rev. Lett.* **106**, 205302 (2011).
- [89] A. Richie-Halford, J. E. Drut, and A. Bulgac, Emergence of a Pseudogap in the BCS-BEC Crossover, *Phys. Rev. Lett.* **125**, 060403 (2020).
- [90] A. Bulgac and G. F. Bertsch, Collective Oscillations of a Trapped Fermi Gas near the Unitary Limit, *Phys. Rev. Lett.* **94**, 070401 (2005).
- [91] G. E. Astrakharchik, J. Boronat, J. Casulleras, and S. Giorgini, Equation of State of a Fermi Gas in the BEC-BCS Crossover: A Quantum Monte Carlo Study, *Phys. Rev. Lett.* **93**, 200404 (2004).
- [92] S. Y. Chang, V. R. Pandharipande, J. Carlson, and K. E. Schmidt, Quantum Monte Carlo studies of superfluid Fermi gases, *Phys. Rev. A* **70**, 043602 (2004).
- [93] P. Hohenberg and W. Kohn, Inhomogeneous electron gas, *Phys. Rev.* **136**, B864 (1964).
- [94] W. Kohn and L. J. Sham, Self-consistent equations including exchange and correlation effects, *Phys. Rev.* **140**, A1133 (1965).
- [95] A. Bulgac, Entropy, single-particle occupation probabilities, and short-range correlations, [arXiv:2203.12079](https://arxiv.org/abs/2203.12079).
- [96] A. Bulgac, Time-dependent density functional theory and the real-time dynamics of Fermi superfluids, *Annu. Rev. Nucl. Part. Sci.* **63**, 97 (2013).
- [97] A. Bulgac, Time-dependent density functional theory for fermionic superfluids: From cold atomic gases, to nuclei and neutron star crust, *Phys. Status Solidi B* **256**, 1800592 (2019).
- [98] A. Bulgac, P. Magierski, K. J. Roche, and I. Stetcu, Induced Fission of  $^{240}\text{Pu}$  Within a Real-Time Microscopic Framework, *Phys. Rev. Lett.* **116**, 122504 (2016).
- [99] A. Bulgac, S. Jin, K. J. Roche, N. Schunck, and I. Stetcu, Fission dynamics of  $^{240}\text{Pu}$  from saddle to scission and beyond, *Phys. Rev. C* **100**, 034615 (2019).
- [100] A. Bulgac, S. Jin, and I. Stetcu, Nuclear fission dynamics: Past, present, needs, and future, *Front. Phys.* **8**, 63 (2020).
- [101] E. R. Davidson, Properties and uses of natural orbitals, *Rev. Mod. Phys.* **44**, 451 (1972).
- [102] A. Bulgac and S. Yoon, Large Amplitude Dynamics of the Pairing Correlations in a Unitary Fermi Gas, *Phys. Rev. Lett.* **102**, 085302 (2009).
- [103] A. Bulgac, Y.-L. Luo, P. Magierski, K. J. Roche, and Y. Yu, Real-time dynamics of quantized vortices in a unitary Fermi superfluid, *Science* **332**, 1288 (2011).
- [104] A. Bulgac, M. M. Forbes, and P. Magierski, The unitary Fermi gas: From Monte Carlo to density functionals, Vol. 836, Chap. 9, pp. 127–191, of [56] (2012).
- [105] A. Bulgac and S. Jin, Dynamics of Fragmented Condensates and Macroscopic Entanglement, *Phys. Rev. Lett.* **119**, 052501 (2017).
- [106] P. Magierski, A. Makowski, M. C. Barton, K. Sekizawa, and G. Wlazłowski, Pairing dynamics and solitonic excitations in collisions of medium-mass, identical nuclei, *Phys. Rev. C* **105**, 064602 (2022).